IRX4204 Induces Senescence and Cell Death in HER2-positive Breast Cancer and Synergizes with Anti-HER2 Therapy

Cassandra L. Moyer[1], Amanda Lanier[1], Jing Qian[1], Darian Coleman[1], Jamal Hill[1], Vidyasagar Vuligonda[2], Martin E. Sanders[2], Abhijit Mazumdar[1], and Powel H. Brown[1,3]

ABSTRACT

Purpose: Rexinoids, agonists of nuclear retinoid X receptor (RXR), have been used for the treatment of cancers and are well tolerated in both animals and humans. However, the usefulness of rexinoids in treatment of breast cancer remains unknown. This study examines the efficacy of IRX4204, a highly specific rexinoid, in breast cancer cell lines and preclinical models to identify a biomarker for response and potential mechanism of action.

Experimental Design: IRX4204 effects on breast cancer cell growth and viability were determined using cell lines, syngeneic mouse models, and primary patient-derived xenograft (PDX) tumors. *In vitro* assays of cell cycle, apoptosis, senescence, and lipid metabolism were used to uncover a potential mechanism of action. Standard anti-HER2 therapies were screened in combination with IRX4204 on a panel of breast cancer cell lines to determine drug synergy.

Results: IRX4204 significantly inhibits the growth of HER2-positive breast cancer cell lines, including trastuzumab and lapatinib–resistant JIMT-1 and HCC1954. Treatment with IRX4204 reduced tumor growth rate in the MMTV-ErbB2 mouse and HER2-positive PDX model by 49% and 44%, respectively. Mechanistic studies revealed IRX4204 modulates lipid metabolism and induces senescence of HER2-positive cells. In addition, IRX4204 demonstrates additivity and synergy with HER2-targeted mAbs, tyrosine kinase inhibitors, and antibody–drug conjugates.

Conclusions: These findings identify HER2 as a biomarker for IRX4204 treatment response and demonstrate a novel use of RXR agonists to synergize with current anti-HER2 therapies. Furthermore, our results suggest that RXR agonists can be useful for the treatment of anti-HER2 resistant and metastatic HER2-positive breast cancer.

Introduction

Nearly 20% of primary breast cancers have overexpression of the HER2, resulting in aggressive tumor growth and poorer clinical prognosis (1, 2). mAbs against HER2 (trastuzumab and pertuzumab) have been highly effective in treating HER2-overexpressing breast cancers by directly blocking growth signals in tumor cells and flagging tumor cells for elimination by the immune system (3–5). Small-molecule tyrosine kinase inhibitors (TKI such as lapatinib, neratinib, and tucatinib) have also been developed to effectively target HER2-amplified primary and metastatic tumors (6–13). More recently, the advancement of monoclonal antibody–drug conjugates (trastuzumab–emtansine and trastuzumab–deruxtecan) has greatly improved the efficacy of HER2-targeted therapies (14, 15).

However, despite the development of highly successful targeted therapies for primary tumors with HER2 amplification, a major problem persists that many patients with recurrent HER2-positive breast cancer acquire resistance to anti-HER2 therapy (16–18). In addition, HER2-targeted therapies have limited ability to cross the blood–brain barrier and women with recurrent HER2-positive tumors often develop brain metastases (19). It is also known that current anti-HER2 therapies exhibit unwanted adverse effects such as cardiotoxicity, hepatic failure, and gastrointestinal complications (20–25). Moreover, most anti–HER2-targeted therapies still fail to achieve a cure in the metastatic setting. There is a critical need for safe and effective therapies that can overcome drug resistance and target breast cancer metastases.

Retinoids and their related molecules, rexinoids, have been used for the treatment of cancers, including acute promyelocytic leukemia, hairy cell leukemia, and Kaposi sarcoma (26, 27). Rexinoids are specific agonists for the nuclear retinoid X receptor (RXR) and can regulate the expression of genes controlling critical signaling pathways and biological functions such as development, metabolism, and inflammation through its dimerization with other partner nuclear receptors like retinoic acid receptor (RAR), liver X receptor (LXR), and peroxisomal proliferator-activated receptor (PPAR). RXR agonists are less toxic than naturally occurring retinoids (which primarily activate RAR transcription factors) and are well tolerated in both animals and humans (28, 29). The third-generation rexinoid, bexarotene, is FDA approved for the treatment of cutaneous T-cell lymphoma and was tested in a phase II clinical trial as a single agent for the treatment of metastatic breast cancer (30, 31). In this trial, bexarotene produced a clinical benefit in roughly 20% of the patients but showed limited efficacy overall in women with refractory metastatic breast cancer. The novel RXR agonist 9cUAB30 has also been shown to decrease tumor growth and increase survival in preclinical models of cancer (32, 33). Notably, 9cUAB30 exhibits fewer toxicities than bexarotene (34). An ongoing phase I trial of 9cUAB30 is currently assessing antitumor effects in early-stage breast cancer (NCT02876640).

[1]Department of Clinical Cancer Prevention, The University of Texas MD Anderson Cancer Center, Houston, Texas. [2]Io Therapeutics, Inc., The Woodlands, Texas. [3]Department of Molecular and Cellular Biology, Baylor College of Medicine, Houston, Texas.

Corresponding Author: Powel H. Brown, The University of Texas MD Anderson Cancer Center, 1515 Holcombe Blvd, Houston, TX 77030. E-mail: phbrown@mdanderson.org

Clin Cancer Res 2024;30:1–13

doi: 10.1158/1078-0432.CCR-23-3839

Translational Relevance

HER2-targeted mAbs, tyrosine kinase inhibitors, and antibody–drug conjugates are effective treatments for HER2-amplified primary breast tumors. However, intrinsic and acquired resistance to anti-HER2 therapy is common, and anti–HER2-targeted therapies still fail to achieve a cure in the metastatic setting. This study has uncovered a novel vulnerability of HER2-positive breast cancer through activation of retinoid X receptor (RXR) nuclear receptor. Our results demonstrate that HER2-positive breast cancer, including anti-HER2–resistant breast cancer, can be targeted with RXR agonists. These findings indicate that rexinoids alone, or in combination with current anti-HER2 therapy, are useful for the treatment of HER2-amplifed breast cancer and suggest that RXR agonists can be beneficial for the treatment of resistant or metastatic HER2-positive tumors.

IRX4204 is a fourth-generation, highly specific RXR agonist devoid of any RAR activity and has shown promise in the treatment and prevention of cancer (35–37). Here we demonstrate that IRX4204 can inhibit the growth of HER2-overexpressed breast cancers, including those resistant to anti-HER2 therapy. This inhibitory effect is achieved in part through RXR modulation of lipid metabolism and the induction of senescence in HER2-positive breast cancer. Furthermore, we show that IRX4204 can synergize with current anti-HER2 therapies to further inhibit breast tumor growth. These findings suggest that rexinoids are useful, alone or in combination, for the treatment of HER2-positive breast cancer.

Materials and Methods

Drugs

IRX4204 was obtained from Io Therapeutics, Inc and dissolved in DMSO. A total of 1 μmol/L IRX4204 has been previously established as a physiologically relevant dose. The synthesis and characterization of IRX4204 has been described previously (35). Anti-HER2–targeted therapies were prepared according to manufacturer instructions: lapatinib (GSK 572016), tucatinib (HY-16069, MedChemExpress), trastuzumab, and T-DM1 (Herceptin and Kadcyla stock solutions obtained from MD Anderson pharmacy). The pan-caspase inhibitor Z-VAD-FMK, inhibiting human caspases 1 and 3–10, was obtained from MedChemExpress and dissolved in DMSO.

Cell line culture

MDA-MB-231 (RRID:CVCL_0062), HCC1143 (RRID:CVCL_1245), HCC70 (RRID:CVCL_1270), MCF7 (RRID:CVCL_0031), SkBr3 (RRID:CVCL_0033), AU565 (RRID:CVCL_1074), MDA-MB-361 (RRID:CVCL_0620), HCC1954 (RRID:CVCL_1259), and HCC1419 (RRID:CVCL_1251) were purchased from ATCC and were maintained in DMEM or RPMI medium according to ATCC recommendations. JIMT-1 (RRID:CVCL_2077) was obtained from Leibniz Institute DSMZ. The MDA231-HER2-OE cell line was a generous gift from Dr. Dihua Yu. Murine cell lines were created from tumor models as described previously (38). Growth media for all cell lines was supplemented with 10% FBS, penicillin (100 mg/mL), and streptomycin (100 mg/mL). SKBR3-LR cells were established by twice weekly treatments with increasing doses of lapatinib (up to 200 nmol/L) for 8 months which resulted in the cell line achieving an IC_{50} value of 212 nmol/L. Stock solutions of lapatinib (100 mmol/L; GlaxoSmithKline), were prepared in DMSO (Sigma-Aldrich). For cell authentication, short tandem repeat profiles were performed by the Cytogenetics and Cell Authentication Core at MD Anderson Cancer Center and compared with: (i) known ATCC fingerprints (ATCC.org); (ii) the Cell Line Integrated Molecular Authentication database (CLIMA) version 0.1.200808 (http://bioinformatics.hsanmartino.it/clima2/); and (iii) the MD Anderson fingerprint database. For *Mycoplasma*, the Lonza Mycoplasma Detection Kit (catalog # LT07-418) was applied according to manufacturer instructions.

Cell growth assays

Cells were plated in 96-well plates and incubated at 37°C overnight, then treated with drugs at indicated concentrations. At days 1, 3, 5, 7, and/or 9, plates were fixed, stained with DAPI, and imaged with an ImageXpress Pico (Molecular Devices). Nuclei were segmented and counted at each timepoint by defining a threshold value of pixel intensity over background and object size, using the cell scoring algorithm of the CellReporterXpress Software (Molecular Devices). Statistical differences in cell growth at each day were assessed using the Student t test ($P < 0.05$).

Drug additivity and synergy

Master stock drug solutions were prepared for each drug using complete media, such that the final concentration approximates the reported IC_{50}s in HER2-overexpressed cell lines following 10-fold dilutions (IRX4204, trastuzumab, lapatinib, and tucatinib) and/or 2-fold dilutions (tucatinib and T-DM1) of each drug. Using these master stocks, a volume for volume mixture of each concentration IRX4204 and respective anti-HER2 drugs were prepared with 1% DMSO media as control. Cell lines were treated for a week with each combination and cell counts were obtained on day 7. The combination index (CI) was determined using CompuSyn (39). $\log_{10}$(CI) of less than, equal to, or more than 0 indicates synergy, additivity, and antagonism, respectively. SynergyFinder was used to calculate synergy scores with four synergy models: zero interaction potency (ZIP), Loewe additivity (LOEWE), Bliss independence (BLISS), and highest single agent (HSA; ref. 40). Synergy scores between 0 and 10 are considered additive and scores above 10 are considered synergistic.

In vivo animal studies

These studies were conducted using an MD Anderson Institutional Animal Care and Use Committee–approved animal protocol. Female MMTV-ErbB2 (RRID:IMSR_JAX:002376) transgenic mice were obtained from The Jackson Laboratory. Pieces from an established tumor of a single MMTV-ErbB2 donor mouse were transplanted into the right fourth inguinal mammary fat pad of 6- to 8-week-old MMTV-ErbB2 recipient mice. When tumor size reached 50 to 100 mm^3, mice were divided randomly into three groups and treated 5 days a week with sesame oil, IRX4204 (10 mg/kg), or tucatinib (20 mg/kg) by oral gavage. Xenograft tumor sizes were measured three times a week, and growth rates were compared between groups. Mice were sacrificed when tumor size reached ≥2,000 mm^3. Patient-derived xenograft (PDX) experiments were conducted at Baylor College of Medicine by the PDX Core. Pieces of tumor (2 mm^3 in size) from patients with TNBC and HER2-positive breast cancer were transplanted into 5-week-old female SCID/Beige mice. Two weeks posttransplant, mice were divided randomly into three or four treatment groups ($n = 9$ per group) and treated 5 days a week with vehicle (1% Tween80/4% DMSO/95% PBS) or IRX4204 (3, 10, and 20 mg/kg) by oral gavage. Tumor volume was measured twice weekly, and growth rates were compared between groups. Mice were sacrificed at 29 days posttreatment.

IHC staining

Tumor samples from the MMTV-ErbB2 mice were processed by fixation in a 10% formalin solution and subsequently embedded in paraffin. Hematoxylin-eosin staining and IHC staining of tumor tissue slides was performed at Baylor College of Medicine Breast Center Pathology Core with Ki67 primary antibody (Lab Vision, catalog # RM-9106, RRID:AB_2341197) or Cleaved Caspase-3 [Cell Signaling Technology, catalog # 9664 (also 9664P), RRID:AB_2070042]. Image acquisition was obtained using Aperio ImageScope (Leica Biosystems) and processed with Aperio ImageScope Pathology Slide Viewing Software (Leica Biosystems; RRID:SCR_020993).

Cell cycle analysis

SkBr3 and AU565 cells plated in 30-mm dishes were synchronized with lovastatin (20 μmol/L) for 48 hours. Cells were washed and released with mevalonate (2 mmol/L) in media containing DMSO or IRX4204 (1 μmol/L). Cells were collected at 0, 12, 24, 27, 30, 33, 36, 48, 54, and 60 hours and fixed in ice-cold 70% ethanol. After the collection of all timepoints, cells were washed, stained with propidium iodide (PI), and measured for DNA content with flow cytometry.

Annexin V

Cells were treated with DMSO, IRX4204 (1 μmol/L), or bortezomib (1 μmol/L) for 72 hours. After treatment, cells were washed with cold PBS, resuspended in Annexin V binding buffer, and incubated with FITC-conjugated Annexin V (Beckman Coulter, catalog # IM2375, RRID:AB_130879) and PI for 15 minutes. After staining, cells were analyzed using a Gallios 561 Flow Cytometer (Beckman Coulter). All experiments performed in triplicate.

Senescence β-galactosidase staining and senescence-associated secretory phenotype quantification

Cells were plated in triplicate into 12-well plates. After 10–14 days of treatment, cells were fixed and stained using the Senescence β-Galactosidase Staining Kit (#9860, Cell Signaling Technology) following the kit protocol. Images were obtained on the EVOS XL Core Microscope (Invitrogen) at 40x magnification. For secreted protein quantification, cell lines were treated with doxorubicin (100 nmol/L; 24 hours), DMSO, or IRX4204 (1 μmol/L) for 4 days. Cells were washed and incubated with serum-free media for 24 hours before the supernatants were collected for analyses of secreted proteins. Quantification of secreted proteins was measured using human IL8 (Thermo Fisher Scientific, catalog # 88-8086-22, RRID:AB_2575173), human IL6 (Thermo Fisher Scientific, catalog # 88-7066-22, RRID:AB_2574991), and human GROα/CXCL1 (Thermo Fisher Scientific, catalog # 88-52122-22, RRID:AB_3083784) ELISA kits according to the manufacturers' instructions. Final concentrations of secreted proteins were normalized to the total number of cells present when supernatants were collected.

Oil Red O staining

Cells were cultured in media containing DMSO or IRX4204 (1 μmol/L) for 72 hours. After treatment, cells were washed and fixed with 10% formalin for at least 1 hour. After fixation, cells were washed with ddH_2O followed by a 5-minute incubation with 60% isopropanol. Cells were completely dried before staining with Oil Red O working solution (O-0625, Sigma) for 10 minutes at room temperature. Cells were washed multiple times with double-distilled H_2O before imaging on an Eclipse Ti2 Microscope (Nikon) at 40x magnification and processed using NIS-Elements (Nikon; RRID:SCR_014329). To quantify lipid accumulation, cells were destained with 100% isopropanol for 10 minutes and optical density (OD) was measured at 500 nmol/L. Six biologic replicates were tested for each cell line and treatment condition.

qRT-PCR

Total RNA was isolated from cells using the RNeasy Mini Kit (74104; Qiagen). After reverse transcription, qRT-PCR was performed on an ABI 7500 System (Applied Biosystems). Relative gene expression was determined using the comparative Ct method and normalized to cyclophilin ($2-\Delta\Delta Ct$ method). Results are shown as the mean relative expression of three biologic replicates. Changes in expression over time were compared using ANOVA statistical analysis with a P value less than 0.05 considered statistically significant. Primer and probe sequences for qRT-PCR analysis are listed in Supplementary Table S1.

Western blots

Cell lines were plated in triplicate, treated with DMSO or IRX4204 (1 μmol/L), and collected for total protein after 4 days. Protein lysates were isolated in RIPA buffer containing protease and phosphatase inhibitors and quantified by bicinchoninic acid assay. A total of 30 μg of total protein was loaded onto 10% SDS-PAGE with molecular markers and run at 80 V for 2 hours. Proteins were transferred at 75 V for 90 minutes to nitrocellulose membranes (Millipore Sigma) using standard wet tank methods. Membranes were blocked with 5% milk in TBS-Tween (0.1%) and probed overnight at 4°C with primary antibodies vinculin 1:2,000 (Sigma-Aldrich, catalog # V9131, RRID:AB_477629), actin 1:1,000 (Sigma-Aldrich, catalog # A2066, RRID:AB_476693), Phospho-Rb S807/811 1:1,000 (Cell Signaling Technology, catalog # 8516, RRID:AB_11178658), and p53 1:1,000 (Santa Cruz Biotechnology, catalog # sc-126, RRID:AB_628082). Membranes were washed with TBS-Tween and probed with anti-mouse and anti-rabbit horseradish peroxidase–linked secondary antibodies (1:1,000, Cell Signaling Technology) for 1 hour before final washing with TBS-Tween. Proteins were visualized using SuperSignal West Fempto Maximum Sensitivity Substrate (Thermo Fisher Scientific) and membranes were imaged using the Bio-Rad ChemiDoc MP Imaging System. Relative protein expression was quantified by measuring densitometry with ImageJ software (RRID:SCR_003070), normalizing values to loading controls and calculating a ratio of protein expression between IRX4204-treated samples and DMSO for each biologic replicate.

Statistical analyses

All graphs are presented as mean ± SD of three or more biological replicates. Two-tailed Student t tests were used to determine the statistical significance between two different groups, and one-way ANOVA tests were used to determine the statistical significance among multiple groups. A P value less than 0.05 is considered statistically significant, with symbols used to represent levels of significance: *, $P \le 0.05$; **, $P \le 0.01$; ***, $P \le 0.001$; ****, $P \le 0.0001$.

Data availability

The data generated in this study are available upon request from the corresponding author.

Results

IRX4204 inhibits the growth of HER2-amplified breast cancer cell lines *in vitro*

To investigate the effects of the RXR agonist IRX4204 on the growth of breast cancer, we treated a panel of human breast cancer cell lines with IRX4204 or DMSO for 1 week and measured cell number over

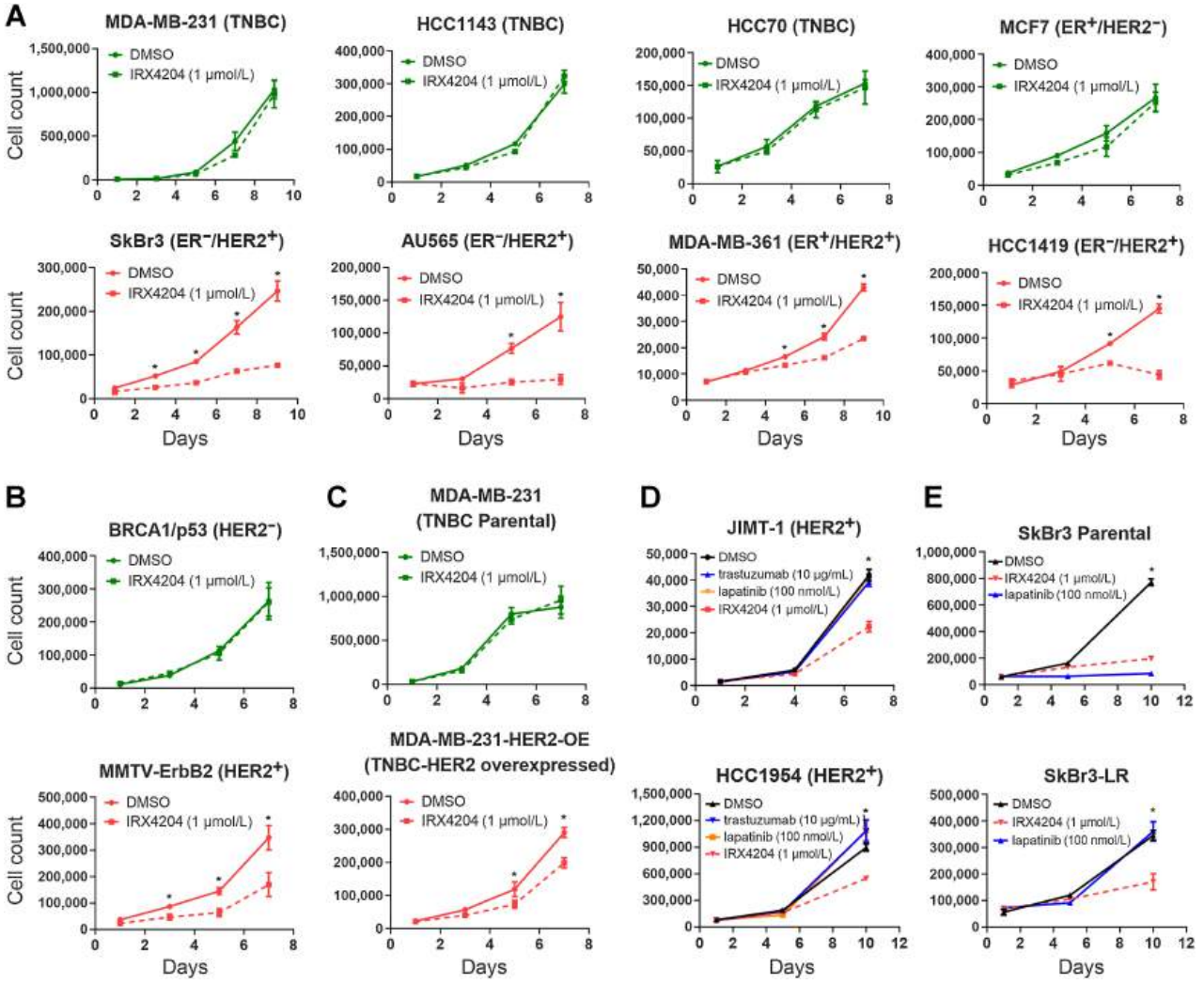

Figure 1.

Effect of IRX4204 on growth of breast cancer cell lines *in vitro*. **A,** Cell growth of four human HER2-negative breast cancer cell lines and four human HER2-positive cell lines treated with IRX4204 (1 μmol/L) or DMSO (control) for 7–9 days. **B,** Cell growth of murine *BRCA1*$^{co/co}$/MMTV-Cre$^{+/+}$/p53$^{+/-}$ (HER2-negative) and MMTV-ErbB2 (HER2-positive) cell lines treated with IRX4204 (1 μmol/L) or DMSO for 7 days. **C,** Cell growth of HER2-normal MDA231 parental cell line and engineered HER2-overexpressed MDA231 cell line treated with IRX4204 (1 μmol/L) or DMSO for 7 days. **D,** Cell growth of JIMT-1 human HER2-positive breast cancer cell line with trastuzumab (10 μg/mL), lapatinib (100 nmol/L), IRX4204 (1 μmol/L), or DMSO for 7 days. **E,** Cell growth of SkBr3 (HER2-positive) and SkBr3-LR cell lines with lapatinib (100 nmol/L), IRX4204 (1 μmol/L), or DMSO for 7 days. Statistical significance was determined using the Bonferroni–Dunn method of multiple *t* tests. Each day was analyzed individually, without assuming a constant SD (*, $P < 0.01$).

time. HER2-amplified breast cancer cell lines (SkBr3, AU565, MDA-MB-361, and HCC1419) exhibited a significant decrease in cell growth upon treatment with IRX4204 compared with DMSO, whereas breast cancer cell lines without HER2 amplification (TNBC cell lines, MDA-MB-231, HCC70, HCC1143, and estrogen receptor–positive/HER2-negative MCF7) showed no change in cell growth (**Fig. 1A**; Supplementary Fig. S1A). We observed similar findings when we treated murine breast cancer cell lines derived from tumors arising in *BRCA1*$^{co/co}$; MMTVCre$^{+/+}$;p53$^{+/-}$ TNBC mouse model (41) and MMTV-ErbB2 HER2-amplified mouse model. Only the HER2-amplified murine tumor line showed sensitivity to IRX4204 treatment (**Fig. 1B**). To further understand the relationship between HER2 expression and RXR activation, we tested the effects of IRX4204 on the growth of TNBC cell line MDA-MB-231 engineered to overexpress HER2 (MDA-MB-231-HER2-OE). We observed a modest inhibition of MDA-MB-231-HER2-OE cell line growth upon treatment with IRX4204 compared with MDA-MB-231 parental cell line (**Fig. 1C**; Supplementary Fig. S1B) indicating that HER2 overexpression can sensitize breast cancer cells to the inhibitory effects of RXR agonists.

To determine the effects of IRX4204 on the growth of anti-HER2 therapy–resistant breast cancer, we treated two breast cancer cell lines resistant to HER2 therapy (JIMT-1 and HCC1954) with IRX4204 (1 μmol/L), trastuzumab (10 μg/mL), lapatinib (100 nmol/L), or DMSO. Only the IRX4204 treatment caused a significant decrease in the growth of resistant breast cancer cells (**Fig. 1D**). In addition, we created a SkBr3 cell line with acquired resistance to lapatinib (SkBr3-LR) by maintaining the cell line in high levels of lapatinib for 8 months (Supplementary Fig. S2). Like JIMT-1 and HCC1954, the SkBr3-LR

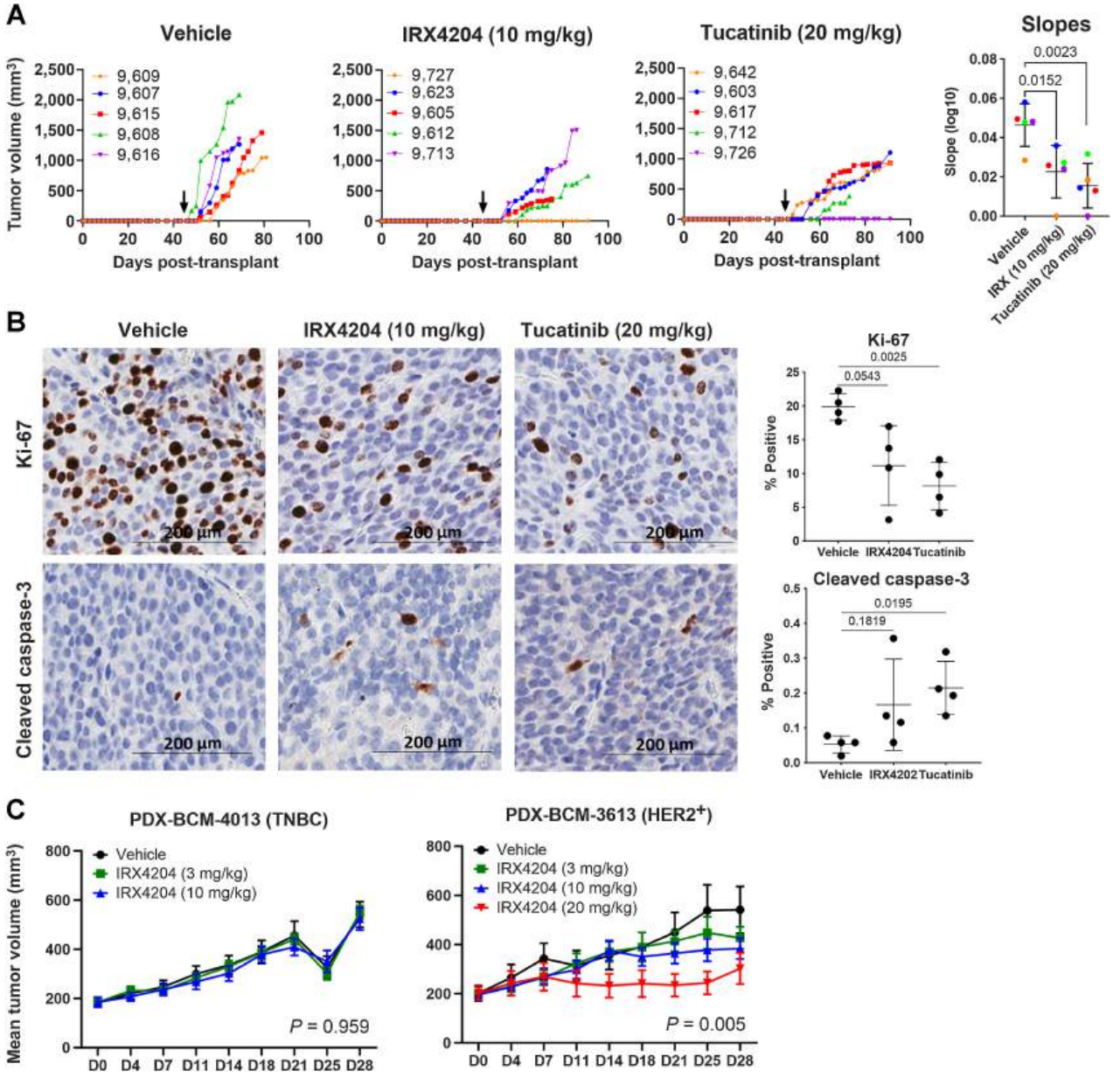

Figure 2.

Effect of IRX4204 on the growth of HER2-amplified breast cancer *in vivo*. **A,** Tumor growth of MMTV-ErbB2 syngeneic transplants with vehicle, IRX4204 (10 mg/kg), or tucatinib (20 mg/kg; $n = 5$ for each group). Statistical significance between the slopes of vehicle and treatment groups was determined using Student *t* test. **B,** Ki-67 and cleaved-caspase 3 IHC of representative tumors from each treatment group. Five different sections of four treated tumors were analyzed from each treatment group using an unpaired *t* test with Welch correction. **C,** PDX tumor growth of TNBC (left) and HER2-positive (right) breast cancer with IRX4204 (3, 10, or 20 mg/kg) or vehicle ($n = 7$ per treatment group). Statistical significance was determined using one-way ANOVA.

cell line maintains sensitivity to IRX4204 after developing resistance to anti-HER2 therapy (**Fig. 1E**).

IRX4204 inhibits the growth of HER2-amplified breast cancer cell lines *in vivo*

To determine the effect of IRX4204 on *in vivo* tumor growth, we transplanted HER2-overexpressed mammary tumors from donor MMTV-ErbB2 transgenic mice into syngeneic MMTV-ErbB2 recipient mice. Forty-five days posttransplant, when palpable tumors had formed, mice were randomized into treatment groups [IRX4204 (10 mg/kg), tucatinib (20 mg/kg), or vehicle]. Mice treated with IRX4204 showed a significant decrease in tumor growth rate compared with mice treated with vehicle and showed a similar decrease in tumor growth rate as mice treated with the anti-HER2 TKI, tucatinib (**Fig. 2A**). Upon IHC evaluation of the tumors, the change in tumor growth rate was accompanied by decreased Ki-67 (decreased proliferation) and increased cleaved caspase 3 staining (increased cell death) in drug-treated tumors compared with vehicle (**Fig. 2B**). These results

suggest that IRX4204 can modestly decrease proliferation and induce apoptosis *in vivo*.

To determine the effect of IRX4204 on human breast cancer tumor growth, established PDXs from a triple-negative breast cancer (PDX-BCM-4013) and HER2-positive breast cancer (PDX-BCM-3613) were treated with IRX4204 at 3, 10, or 20 mg/kg. Only the HER2-overexpressed PDX tumors showed a dose-dependent decrease in tumor growth upon IRX4204 treatment (**Fig. 2C**).

IRX4204 induces cell death through apoptosis and cellular senescence of HER2-amplifed breast cancer

Previously, our research group has shown that the rexinoid bexarotene can repress cyclin D1 transcription *in vitro* and *in vivo* (42). To determine whether growth inhibition by IRX4204 is also linked to cell cycle regulation, we first assessed the effects of IRX4204 on cell cycle progression. HER2-amplified SkBr3 and AU565 cells were synchronized with lovastatin and released with mevalonate and IRX4204 (1 μmol/L) or DMSO, followed by DNA content analysis over time for 60 hours. At each timepoint, we observed similar percentages of cells in G_1-, S-, or G_2-phase between IRX4204 and DMSO treatment, suggesting that IRX4204 does not cause an immediate delay in progression through the cell cycle (**Fig. 3A**; Supplementary Fig. S3).

To determine whether IRX4204 induces apoptosis in HER2-positive cell lines, we measured Annexin V-PI induction with DMSO, IRX4204, and bortezomib as a positive control. As expected, all cell lines showed an increase in Annexin V and/or PI upon treatment with bortezomib compared with DMSO control. We also observed a significant increase of PI positivity in the HER2-positive SkBr3 and AU565 cell lines, but not in HER2-normal MCF7, after IRX4204 treatment, indicating IRX4204 can induce cell death in HER2-amplified cell lines. We also observed a modest increase of Annexin V positivity in AU565 cells but not in SkBr3 (**Fig. 3B**). In addition, when the HER2-amplified cell lines were treated with both IRX4204 and the pan-caspase apoptosis inhibitor, Z-VAD, there was a slight rescue in cell growth (Supplementary Fig. S4). These findings suggest that although apoptosis is occurring in IRX4204-treated HER2-positive cell lines, apoptotic death alone cannot fully explain the observed decrease in cell growth after IRX4204 treatment.

Upon IRX4204 treatment, we consistently observed enlarged cells with abnormal morphology in many of the HER2-amplified cell lines. At 6 days after treatment, we measured the induction of senescence by beta-galactosidase (beta-gal) staining and expression of senescence-associated proteins, p53, and phosphorylated Rb protein. HER2-amplifed cell lines, SkBr3, AU565, and MDA361 show increased beta-gal staining with a corresponding decrease in phosphorylated Rb after IRX4204 treatment, whereas HER2-normal cell lines, MCF7 and MDA231 did not (**Fig. 3C**; Supplementary Fig. S5). Notably, we did not see changes in p53 expression after IRX4204 treatment in the HER2-positive cells lines or the HER2-normal MDA231 cell line, suggesting senescence is not induced via the p53 pathway. Although IRX4204 treatment does appear to decrease the expression p53 in the HER2-normal MCF7 cell line, it does not affect MCF7 growth.

To further explore this senescence phenotype, we assessed changes in the expression of senescence-associated secretory proteins (SASP) by measuring secreted IL6, IL8, and GROα levels in the media after 4 days of treatment with IRX4204 (1 μmol/L) or the chemotherapy doxorubicin (100 nmol/L). As expected, treatment with doxorubicin increased the secretion of senescence-associated proteins from all cell lines tested. But only HER2-positive cell lines (SkBr3, AU565, and MDA361) show a significant increase in the secretion of IL6, IL8, and/or GROα after treatment with IRX4204 compared with DMSO control (**Fig. 3D**).

IRX4204 modulates lipid metabolism in HER2-amplified breast cancer

Because it is known that lipid metabolism is frequently altered in HER2-positive breast cancer (43–45) and RXR agonists can modulate lipogenesis (46), we sought to investigate the effects of IRX4204 on lipid metabolism of HER2-overexpressing cell lines. At 48 hours of IRX4204 treatment, staining with Oil Red O revealed an increased lipid production in the HER2-overexpressing SkBr3, AU565, and MDA361, but not in HER2-normal, MCF7, or MDA231 cell lines (**Fig. 4A**). Because RXR can dimerize with the nuclear LXR to modulate lipid metabolism through the regulation of *SREBP-1c* transcription (47), we measured gene expression at multiple timepoints within 24 hours of IRX4204 treatment. We observed an immediate increase of *SREBP-1c* transcript, and its downstream target *FASN*, in HER2-amplified cell lines, SkBr3, AU565, and MDA361. In contrast, an increase in *SREBP-1c* expression, but not *FASN*, was observed in the IRX4204-treated HER2-normal MDA-MB-231 cells and neither *SREBP-1c* or *FASN* gene expression significantly changed in the HER2-normal MCF7 cell line (**Fig. 4B**).

IRX4204 synergizes with anti-HER2 therapy to inhibit cell growth *in vitro*

Because IRX4204 preferentially affects HER2-amplified breast cancer, we sought to determine the effects of IRX4204 with current therapies for HER2-positive breast cancer. We treated breast cancer cell lines with IRX4204 in combination with anti-HER2 mAb therapy, trastuzumab, TKIs, lapatinib and tucatinib, and the monoclonal antibody–drug conjugate, T-DM1 (trastuzumab emtansine) *in vitro* and measured cell growth. Cell lines that are sensitive to IRX4204 alone (AU565, SkBr3, MDA361) showed further cell growth inhibition when anti-HER2 therapies were added, compared with resistant cells (MCF7, MDA231) which did not exhibit changes in cell growth to any of the targeted therapies (**Fig. 5A**; Supplementary Fig. S6A). Similar observations were made when IRX4204 was combined with chemotherapies, paclitaxel, and doxorubicin. HER2-amplified cell line growth is inhibited more when IRX4204 is added to chemotherapy while HER2-normal cell lines are only inhibited by chemotherapy alone (Supplementary Fig. S6B).

To determine whether IRX4204 is additive or synergistic with anti-HER2 therapy, we performed an 8 by 8 drug dose combination of IRX4204 with tucatinib and a 4 by 5 drug dose combination of IRX4204 with TDM-1 on HER2-overexpressed AU565, SkBr3, and MDA361 cells. A CI was calculated for each dose combination compared with the effects of each single agent alone. Most of the dose combinations tested showed synergy [$\log_{10}$(CI) below zero] or additivity [$\log_{10}$(CI) near zero] in the treatment of HER2-overexpressed cell lines (**Fig. 5B**; Supplementary Fig. S6C). In addition, we evaluated the synergy potential using four major synergy models: ZIP, LOEWE, BLISS, and HSA (40). Many of the dose combinations tested show that IRX4204 is additive or synergistic (scores above 0 and 10, respectively), with tucatinib and T-DM1 specifically in the LOEWE and HSA models, with overall mean scores ranging from 0.53 to 13.28 and individual dose combination scores reaching upward of 30 in these two models (Supplementary Fig. S7 and S8).

Discussion

Preclinical and clinical studies have shown that RXR agonists can be effective in the treatment of cancer, including in some breast cancer

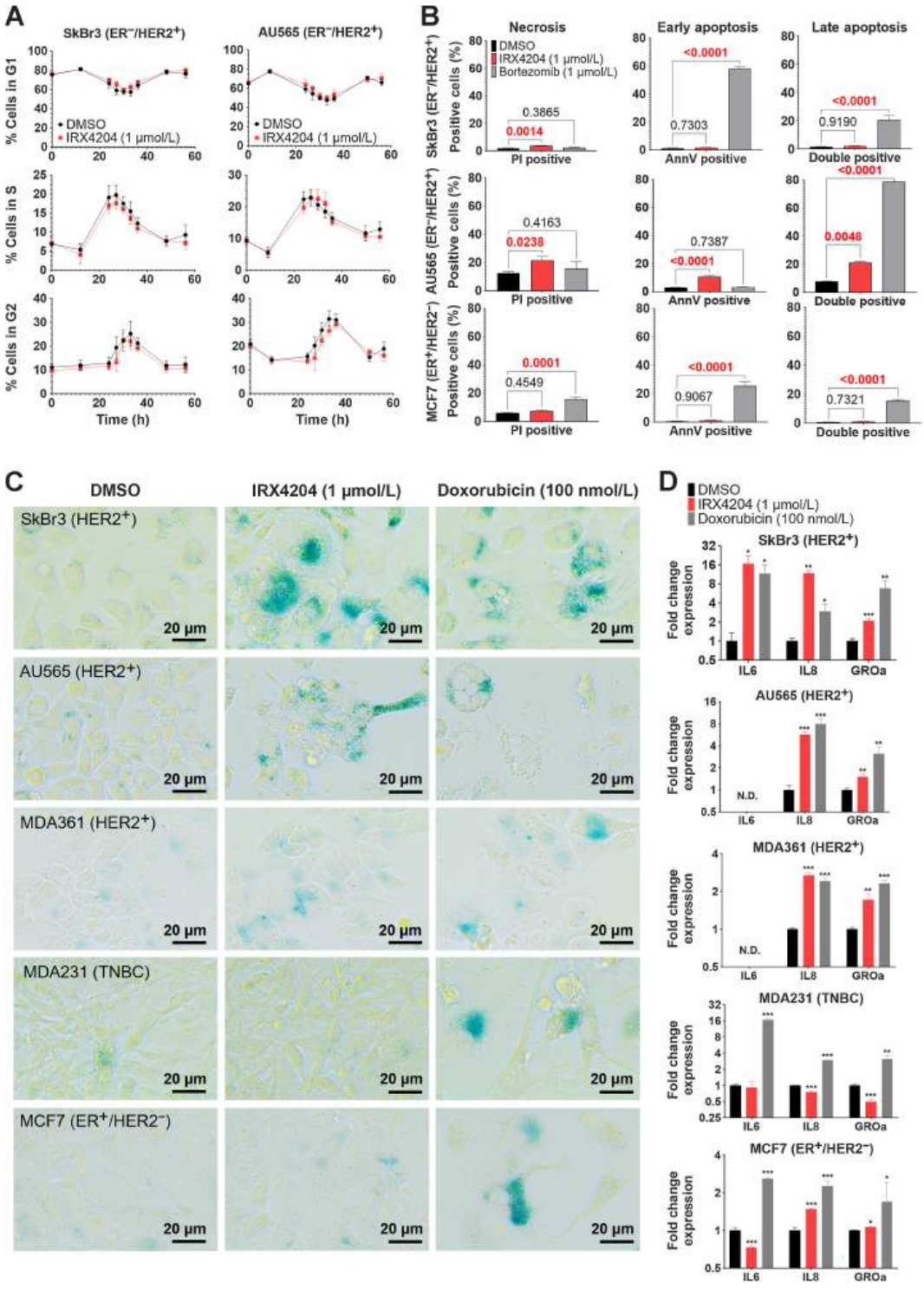

Figure 3.

Cellular effects of IRX4204 on HER2-amplified breast cancer cell lines. **A,** HER2-positive SkBr3 and AU565 cells were blocked in G_1-phase and released with IRX4204 (1 μmol/L) or DMSO treatment. The percentage of cells in G_1-, S-, G_2–M-, and sub-G_1-phases were measured over time by flow cytometry. **B,** Annexin V and PI staining of SkBr3 and AU565 cells treated with IRX4204 (1 μmol/L), bortezomib (1 μmol/L), or DMSO for 72 hours. Statistical significance between groups was determined using Dunnett multiple comparison test. **C,** Beta-gal staining of a panel of human breast cancer cell lines treated with DMSO, IRX4204 (1 μmol/L), or doxorubicin (100 nmol/L) for 6 days. **D,** IL6, IL8, and GROα expression of SkBr3, AU565, MDA361, MDA231, and MCF7 cells with DMSO, IRX4204 (1 μmol/L), or doxorubicin (100 nmol/L) for 4 days. Statistical significance was determined using Welch *t* test. ND (not detected) represents values below detectable limits of the ELISA.

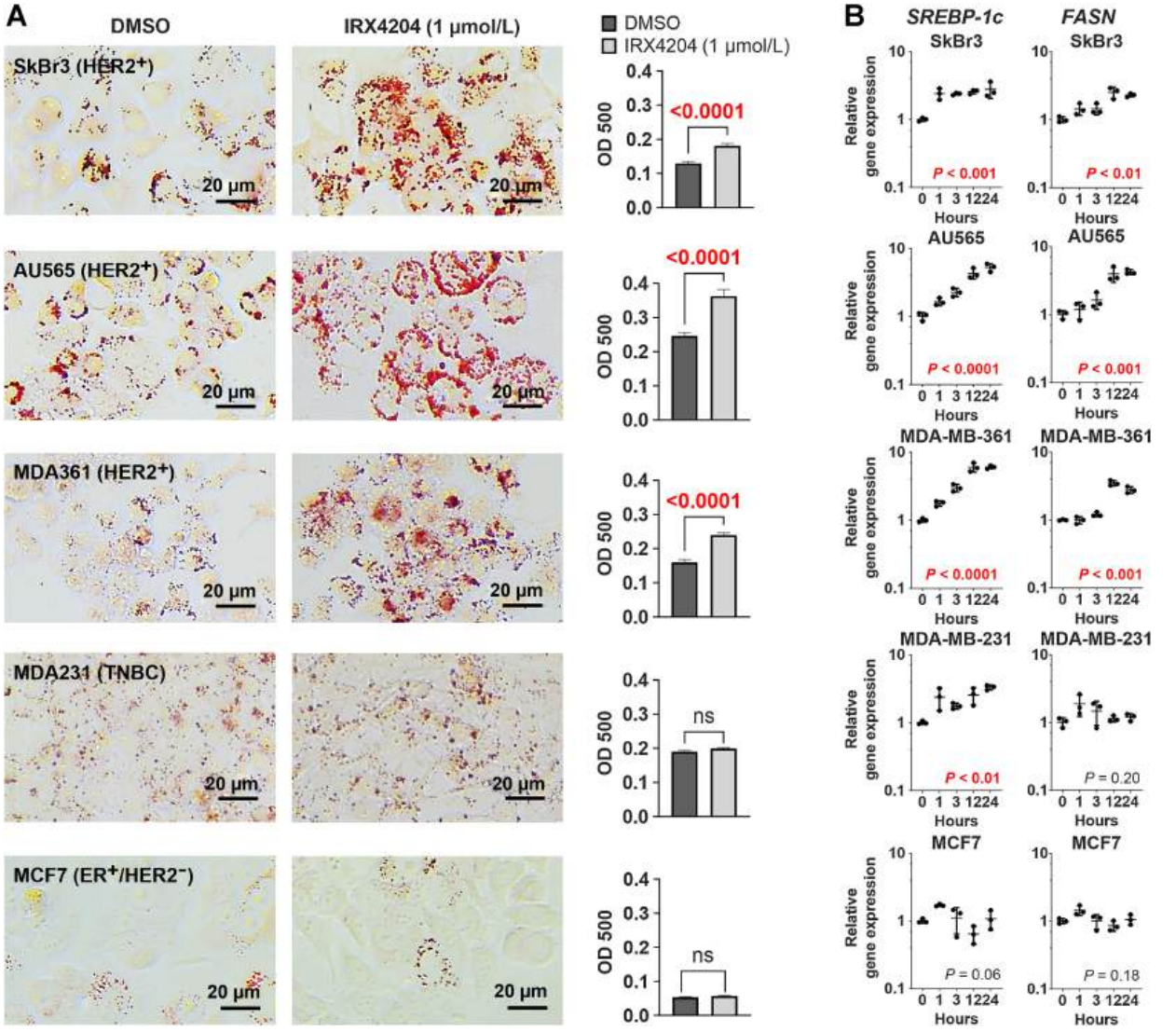

Figure 4.

The effect of IRX4204 on lipid metabolism of HER2-amplified breast cancer. **A,** Oil Red O staining of a panel of human breast cancer cell lines treated with DMSO or IRX4204 (1 μmol/L) for 48 hours. After imaging, cells were destained and total Oil Red O was measured by absorbance at 500 nm. Statistical significance was determined using Welch *t* test. **B,** *SREBP-1c* and *FASN* expression of SkBr3, AU565, MDA361, MDA231, and MCF7 cells at 0, 1, 3, 12, and 24 hours of IRX4204 treatment. Statistical significance was determined using one-way ANOVA.

models (32, 33, 48, 49). In this study, we sought to identify a predictive biomarker for rexinoid activity. Our results demonstrate that the RXR agonist IRX4204 preferentially inhibits the growth of HER2-overexpressed breast cancer, including anti-HER2–resistant cell lines, syngeneic HER2-amplified mouse tumors, and HER2-positive PDX tumors. To explain this inhibitory effect, we found that treatment with IRX4204 alters lipid metabolism in cell lines overexpressing HER2, accompanied by a release of inflammatory cytokines, induction of senescence, and cell death. We also show that IRX4204 can synergize with current HER2-targeted therapies to inhibit the growth of HER2-overexpressing breast cancer cell lines more than single agent alone.

On the basis of our results, we propose a potential mechanism by which treatment with IRX4204 modulates lipid metabolism and induces cellular senescence in HER2-positive breast cancer, ultimately leading to cell death. Breast cancer cells with normal HER2 expression have relatively normal expression of fatty acids and lipid metabolism genes (**Fig. 6**, top left). When HER2-normal cells were treated with IRX4204, we observed no changes in lipid metabolism and no effect on cellular growth (**Fig. 6**, top right). In contrast, it is known that HER2-positive breast cancer cells have increased levels of *de novo* fatty acid synthesis compared with HER2-normal cells (ref. 43; **Fig. 6**, bottom left). When HER2-amplified cells were treated with IRX4204, we observed increased lipid droplet formation, increased *SREBP-1c* and *FASN* expression, increased cellular senescence with release of inflammatory cytokines, and increased apoptotic and necrotic cell death (**Fig. 6**, bottom right).

It is known that the growth of HER2-overexpressing breast cancer can be dependent on *de novo* biosynthesis of fatty acids and that aberrant lipid metabolism can contribute to anti-HER2 treatment resistance (50). In part, this is due to a positive feedback loop between

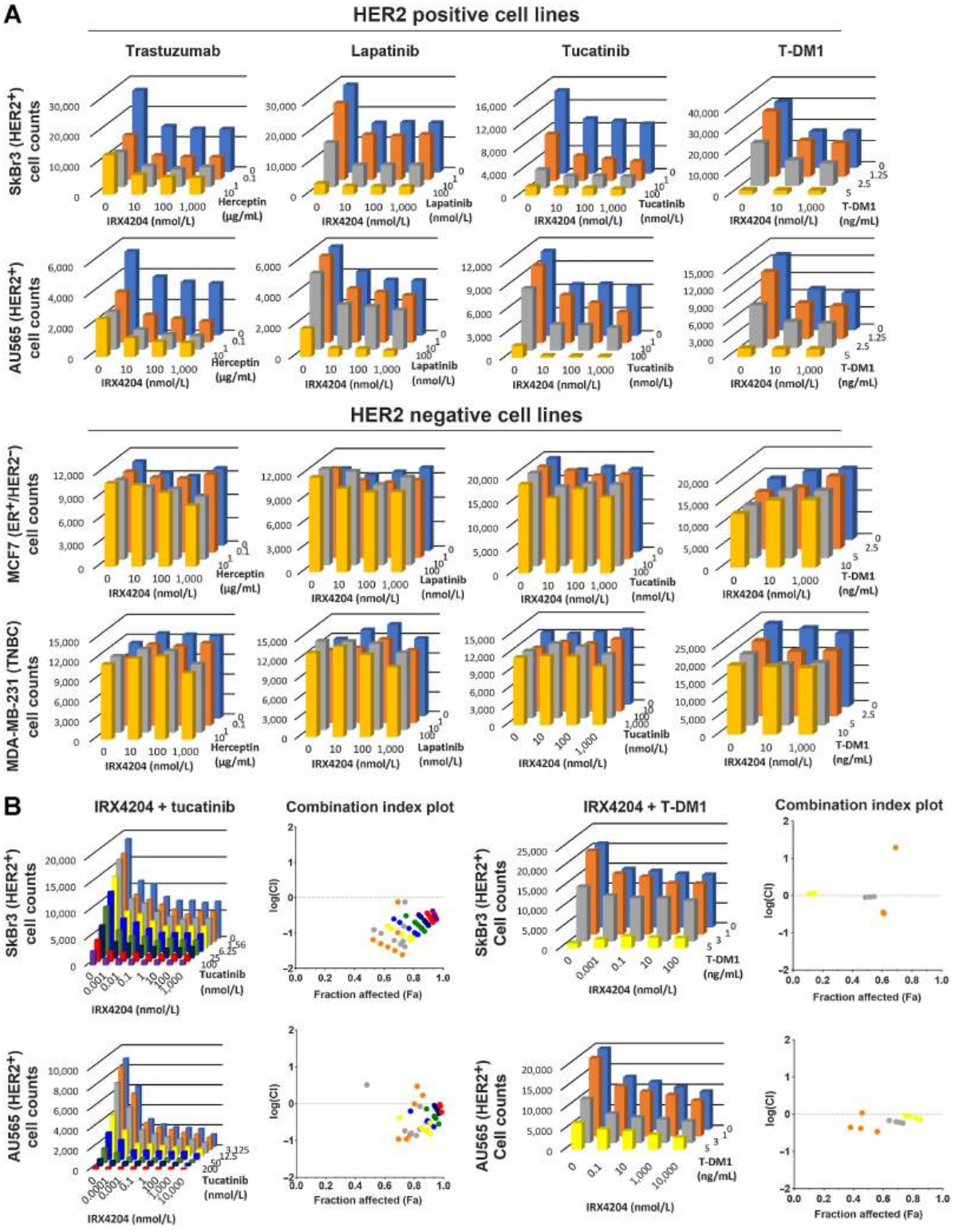

Figure 5.

Synergy of IRX4204 with anti-HER2 therapy *in vitro*. **A,** Nuclei counts of HER2-positive SkBr3 and AU565 and HER2-negative MCF7 and MDA231 cell lines treated with IRX4204 (0, 10, 100, 1,000 nmol/L) in combination with increasing doses of anti-HER2 therapies (trastuzumab, lapatinib, tucatinib, and T-DM1) for 7 days. **B,** Nuclei counts of SkBr3 (top) and AU565 (bottom) treated with increasing doses of IRX4204 in combination with increasing doses of tucatinib (left) or T-DM1 (right) at increasing concentrations. The CI value for each dose combination [log (CI)] is plotted against the fraction of cells affected (Fa). Datapoints near log (CI) = 0 represent drug additivity and less than zero represent drug synergy. For all drug combination experiments, the average nuclei count of 6 replicates for each combination is displayed. SD among replicates is less than 8% in all cases.

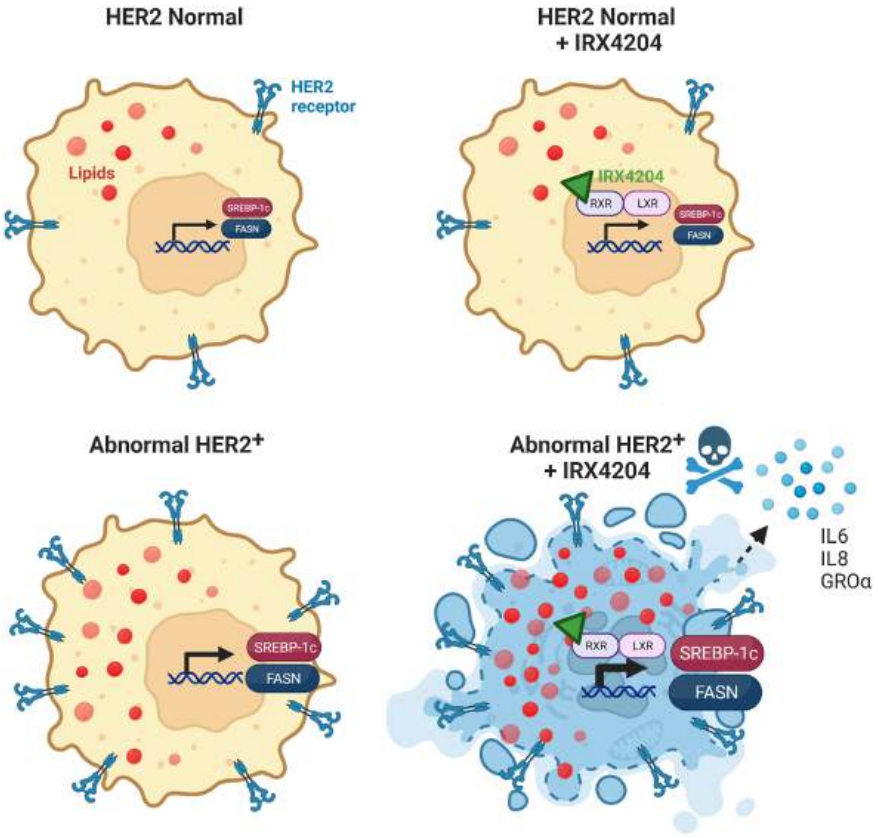

Figure 6.
Mechanism by which IRX4204 induces cell death in HER2-amplifed breast cancer cells. Breast cancer cells expressing normal levels of HER2 have lower levels of lipid metabolism and fewer lipid droplets than cells with HER2 overexpression (left). When treated with the RXR agonist, IRX4204, HER2-normal breast cancer cells show minimal changes in lipid metabolism gene expression or lipid droplet formation (top right). In contrast, HER2 amplified breast cancer cells treated with IRX4204 show increased expression of lipid metabolism genes, increased lipid droplet formation, increased beta-gal staining, and increased secretion of SASPs, resulting in the death of the cell (bottom right). (Figure created with BioRender.com.)

FASN and HER2 which drives HER2-positive breast cancer proliferation via metabolic reprogramming (51). RXR heterodimeric partners, LXR and PPAR, can also regulate the synthesis of fatty acids and have been implicated in the metabolic control of cancers (52–54). Indeed, many studies have shown that LXR- and PPAR-specific agonists can inhibit proliferation and induce apoptosis of breast cancer cell lines (55–57) and RXR agonists are known to activate LXR and PPAR transcription of lipid metabolism–associated genes (47). Our study reveals that IRX4204 can also regulate lipid metabolism and inhibit the growth of HER2-positive breast cancer. Together, these findings suggest that RXR agonists may further exacerbate lipogenesis in HER2-overxpressing breast cancer, including those resistant to conventional anti-HER2 therapy, to induce senescence, ultimately causing cell death.

As an RXR nuclear receptor agonist, the primary function of IRX4204 is to modulate gene transcription. Our study demonstrates immediate changes in gene expression of lipid metabolism upon IRX4204 treatment. Because lipid changes are known to drive cellular senescence (58, 59), we now hypothesize that IRX4204 indirectly induces cellular senescence as a late consequence of the disruption of HER2-driven lipid metabolism, as evidenced by the increase in beta-gal activity, decrease in phosphorylated Rb expression and release of SASPs in HER2-overexpressed cell lines. This is also consistent with the observed increase in PI uptake (necrosis) of IRX4204-sensitive cell lines, resulting from senescence-associated changes in membrane structure and fluidity. Although IRX4204 induces apoptosis in some HER2-overexpressed breast cancer cell lines, the changes are minimal and the inhibitory effect of IRX4204 could not be rescued with the addition of a pan-caspase apoptosis inhibitor. These findings suggest that apoptosis is not the primary effect of IRX4204 inhibition and align with the known role of senescence to protect cells from apoptosis (60). Because the induction of senescence is a late effect, growth arrest in G_1-phase would likely not be observed in the first cell cycle upon treatment with IRX4204. This is consistent with our results that IRX4204 does not arrest cell cycle immediately following treatment. However, the decrease in phosphorylated Rb observed after 4 days of IRX4204 treatment corroborates a late-stage senescence-associated cell cycle arrest.

Cellular senescence is a common consequence of anticancer therapies and plays an important role in tumor suppression through irreversible growth arrest of tumor cells. However, senescence can also promote tissue repair and increase inflammation associated with cancer progression. In fact, anti-HER2 therapies have been shown to induce senescence, which has been linked to possible drug resistance mechanisms (61). However, exploiting senescence for the treatment of cancer has also been of current interest. A recent study demonstrated that the induction of senescence by doxorubicin and palbociclib can enhance the efficacy of HER2-targeted antibody–drug conjugates in breast cancer (62). These findings suggest that the addition of senescence-inducing therapies, such as IRX4204, could amplify the effects of HER2-targeted antibody–drug conjugates. *In vivo* studies to assess the efficacy of IRX4204 in combination with anti-HER2 therapies for the eradication of anti-HER2–resistant and HER2-overexpressed metastatic breast cancer are necessary.

RXR agonists have been shown to modulate the immune system in preclinical models of breast cancer, including those with HER2 overexpression. Liby and colleagues have demonstrated that the RXR agonist, LG100268, can decrease myeloid-derived suppressor cells and CD206-expressing macrophages while increasing PD-L1 expression and the ratio of CD8/CD4-positive T cells in a preclinical model of

HER2-positive breast cancer (63). Similarly, they showed that another RXR agonist, MSU42011, can also increase the percentage of CD8-positive cytotoxic T cells in the same preclinical model (48). Our results show that IRX4204 disrupts lipid regulation, induces senescence, and leads to the release of inflammatory cytokines in HER2-postive breast cancer cell lines. Because lipids and cytokines are known to stimulate the tumor immune response, it is possible that IRX4204 may also synergize with immunotherapy to inhibit breast cancer growth. Future studies are needed to investigate the role of IRX4204 in the antitumor immune response of HER2-overexpressing breast cancers.

An unmet need in HER2-targeted therapies is effective treatment for HER2-positive brain metastases. Conventional anti-HER2 therapies, like mAbs and TKIs, are largely unable to penetrate the blood–brain barrier to effectively eliminate HER2-overxpressing breast cancer that has metastasized to the brain. For this reason, even with HER2-targeted therapy, patients with HER2-positive breast cancer brain metastases have a median overall survival of just 14 months with a 2-year survival of 25% (64). In contrast to anti-HER2 therapy, the RXR agonist IRX4204 can easily permeate the blood–brain barrier and has been studied for the treatment of brain diseases like Parkinson's disease (65, 66). Efforts to test the efficacy of IRX4204 in the prevention and treatment of HER2-overexpressing breast cancer brain metastases are ongoing.

In conclusion, our study has identified a novel vulnerability of HER2-positive breast cancer through activation of the nuclear receptor RXR. Notably, our results demonstrate that HER2-positive breast cancer, including anti-HER2–resistant breast cancer, can be targeted with RXR agonists. Thus far, rexinoids have not been widely used in breast cancer treatment due to limited response in early-phase clinical trials for metastatic disease, which have included all subtypes of breast cancer. Our data imply that HER2 expression can serve as a biomarker to predict response to RXR agonists. Furthermore, our study indicates that rexinoids are effective against anti-HER2–resistant breast cancer and can synergize with current anti-HER2 therapy for the treatment of HER2-amplifed breast cancer. Finally, our findings advocate that rexinoids, with an ability to pass through the blood–brain barrier, should be considered for the treatment of HER2-positive breast cancer brain metastases.

Authors' Disclosures

C.L. Moyer reports a patent for US-11896558-B2 issued to Io Therapeutics and Board of Regents, The University of Texas System, as well as a patent for US-20230172890-A1 pending. V. Vuligonda reports other support from Io Therapeutics, Inc. during the conduct of the study, as well as other support from Io Therapeutics Inc. outside the submitted work; in addition, V. Vuligonda has a patent for Uses of RXR agonist IRX4204 for cancer treatment issued. M.E. Sanders reports other support from Io Therapeutics, Inc. during the conduct of the study, as well as other support from Io Therapeutics, Inc. outside the submitted work; in addition, M.E. Sanders has a patent for Uses of RXR agonist IRX4204 for cancer treatment issued. A. Mazumdar reports a patent for US-11896558-B2 issued to Io Therapeutics, Inc. and Board of Regents, The University of Texas System, Austin, TX, as well as a patent for US-20230172890-A1 pending. P.H. Brown reports other support from GeneTex outside the submitted work. No disclosures were reported by the other authors.

Authors' Contributions

C.L. Moyer: Conceptualization, data curation, formal analysis, writing–original draft, writing–review and editing. **A. Lanier:** Writing–review and editing. **J. Qian:** Writing–review and editing. **D. Coleman:** Data curation, formal analysis, writing–review and editing. **J. Hill:** Data curation, formal analysis, writing–review and editing. **V. Vuligonda:** Writing–review and editing. **M.E. Sanders:** Resources, writing–review and editing. **A. Mazumdar:** Formal analysis, writing–review and editing. **P.H. Brown:** Conceptualization, supervision, funding acquisition, methodology, writing–review and editing.

Acknowledgments

We would like to thank the Flow Cytometry and Cellular Imaging Core Facility North Campus at The University of Texas MD Anderson Cancer Center, for conducting the flow cytometry experiments. We would also like to thank Sam Tillinger and Michelle Savage for their efforts in the submission of the article. This work was funded by a CCSG grant (P30 CA016672, to P.H. Brown), the John Charles Cain Endowment (to P.H. Brown), and the CFP Foundation (Odyssey Fellowship, to C.L. Moyer).

Note

Supplementary data for this article are available at Clinical Cancer Research Online (http://clincancerres.aacrjournals.org/).

Received December 8, 2023; revised March 4, 2024; accepted April 3, 2024; published first April 5, 2024.

References

1. Slamon DJ, Clark GM, Wong SG, Levin WJ, Ullrich A, McGuire WL. Human breast cancer: correlation of relapse and survival with amplification of the HER-2/neu oncogene. Science 1987;235:177–82.
2. Howlader N, Cronin KA, Kurian AW, Andridge R. Differences in breast cancer survival by molecular subtypes in the United States. Cancer Epidemiol Biomarkers Prev 2018;27:619–26.
3. Cobleigh MA, Vogel CL, Tripathy D, Robert NJ, Scholl S, Fehrenbacher L, et al. Multinational study of the efficacy and safety of humanized anti-HER2 monoclonal antibody in women who have HER2-overexpressing metastatic breast cancer that has progressed after chemotherapy for metastatic disease. J Clin Oncol 1999;17:2639–48.
4. Slamon D, Pegram M. Rationale for trastuzumab (Herceptin) in adjuvant breast cancer trials. Semin Oncol 2001;28:13–9.
5. Hudis CA. Trastuzumab–mechanism of action and use in clinical practice. N Engl J Med 2007;357:39–51.
6. Geyer CE, Forster J, Lindquist D, Chan S, Romieu CG, Pienkowski T, et al. Lapatinib plus capecitabine for HER2-positive advanced breast cancer. N Engl J Med 2006;355:2733–43.
7. Baselga J, Bradbury I, Eidtmann H, Di Cosimo S, de Azambuja E, Aura C, et al. Lapatinib with trastuzumab for HER2-positive early breast cancer (NeoALTTO): a randomised, open-label, multicentre, phase 3 trial. Lancet 2012;379:633–40.
8. Harbeck N. Neoadjuvant and adjuvant treatment of patients with HER2-positive early breast cancer. Breast 2022;62:S12–6.
9. Blackwell KL, Burstein HJ, Storniolo AM, Rugo H, Sledge G, Koehler M, et al. Randomized study of lapatinib alone or in combination with trastuzumab in women with ErbB2-positive, trastuzumab-refractory metastatic breast cancer. J Clin Oncol 2010;28:1124–30.
10. Chan A, Moy B, Mansi J, Ejlertsen B, Holmes FA, Chia S, et al. Final efficacy results of neratinib in HER2-positive hormone receptor-positive early-stage breast cancer from the phase III ExteNET trial. Clin Breast Cancer 2021;21:80–91.
11. Martin M, Holmes FA, Ejlertsen B, Delaloge S, Moy B, Iwata H, et al. Neratinib after trastuzumab-based adjuvant therapy in HER2-positive breast cancer (ExteNET): 5-year analysis of a randomised, double-blind, placebo-controlled, phase 3 trial. Lancet Oncol 2017;18:1688–700.
12. Murthy R, Borges VF, Conlin A, Chaves J, Chamberlain M, Gray T, et al. Tucatinib with capecitabine and trastuzumab in advanced HER2-positive metastatic breast cancer with and without brain metastases: a non-randomised, open-label, phase 1b study. Lancet Oncol 2018;19:880–8.
13. Lin NU, Murthy RK, Abramson V, Anders C, Bachelot T, Bedard PL, et al. Tucatinib vs placebo, both in combination with trastuzumab and capecitabine, for previously treated ERBB2 (HER2)-positive metastatic breast cancer in patients with brain metastases: updated exploratory analysis of the HER2CLIMB randomized clinical trial. JAMA Oncol 2023;9:197–205.
14. Dieras V, Miles D, Verma S, Pegram M, Welslau M, Baselga J, et al. Trastuzumab emtansine versus capecitabine plus lapatinib in patients with previously treated HER2-positive advanced breast cancer (EMILIA): a descriptive analysis of final

overall survival results from a randomised, open-label, phase 3 trial. Lancet Oncol 2017;18:732–42.
15. Andre F, Hee Park Y, Kim SB, Takano T, Im SA, Borges G, et al. Trastuzumab deruxtecan versus treatment of physician's choice in patients with HER2-positive metastatic breast cancer (DESTINY-Breast02): a randomised, open-label, multicentre, phase 3 trial. Lancet 2023;401:1773–85.
16. Wilks ST. Potential of overcoming resistance to HER2-targeted therapies through the PI3K/Akt/mTOR pathway. Breast 2015;24:548–55.
17. Choong GM, Cullen GD, O'Sullivan CC. Evolving standards of care and new challenges in the management of HER2-positive breast cancer. CA Cancer J Clin 2020;70:355–74.
18. Zhang Y. The root cause of drug resistance in HER2-positive breast cancer and the therapeutic approaches to overcoming the resistance. Pharmacol Ther 2021; 218:107677.
19. Kennecke H, Yerushalmi R, Woods R, Cheang MC, Voduc D, Speers CH, et al. Metastatic behavior of breast cancer subtypes. J Clin Oncol 2010;28:3271–7.
20. Mohan N, Jiang J, Dokmanovic M, Wu WJ. Trastuzumab-mediated cardiotoxicity: current understanding, challenges, and frontiers. Antib Ther 2018;1:13–7.
21. Al-Dasooqi N, Bowen JM, Gibson RJ, Sullivan T, Lees J, Keefe DM. Trastuzumab induces gastrointestinal side effects in HER2-overexpressing breast cancer patients. Invest New Drugs 2009;27:173–8.
22. Sodergren SC, Copson E, White A, Efficace F, Sprangers M, Fitzsimmons D, et al. Systematic review of the side effects associated with anti-HER2-targeted therapies used in the treatment of breast cancer, on behalf of the EORTC quality of life group. Target Oncol 2016;11:277–92.
23. Cortes J, Fumoleau P, Bianchi GV, Petrella TM, Gelmon K, Pivot X, et al. Pertuzumab monotherapy after trastuzumab-based treatment and subsequent reintroduction of trastuzumab: activity and tolerability in patients with advanced human epidermal growth factor receptor 2-positive breast cancer. J Clin Oncol 2012;30:1594–600.
24. Piccart-Gebhart MJ, Procter M, Leyland-Jones B, Goldhirsch A, Untch M, Smith I, et al. Trastuzumab after adjuvant chemotherapy in HER2-positive breast cancer. N Engl J Med 2005;353:1659–72.
25. Lamot C, Rottey S, De Backer T, Van Bortel L, Robays H, Van Belle S, et al. Cardiac toxicity of trastuzumab: experience at the Ghent University Hospital, Belgium. Acta Clin Belg 2010;65:300–4.
26. Beckenbach L, Baron JM, Merk HF, Loffler H, Amann PM. Retinoid treatment of skin diseases. Eur J Dermatol 2015;25:384–91.
27. Uray IP, Dmitrovsky E, Brown PH. Retinoids and rexinoids in cancer prevention: from laboratory to clinic. Semin Oncol 2016;43:49–64.
28. Stadler R, Kremer A. Therapeutic advances in cutaneous T-cell lymphoma (CTCL): from retinoids to rexinoids. Semin Oncol 2006;33:S7–10.
29. Liby K, Royce DB, Risingsong R, Williams CR, Wood MD, Chandraratna RA, et al. A new rexinoid, NRX194204, prevents carcinogenesis in both the lung and mammary gland. Clin Cancer Res 2007;13:6237–43.
30. Duvic M, Hymes K, Heald P, Breneman D, Martin AG, Myskowski P, et al. Bexarotene is effective and safe for treatment of refractory advanced-stage cutaneous T-cell lymphoma: multinational phase II-III trial results. J Clin Oncol 2001;19:2456–71.
31. Esteva FJ, Glaspy J, Baidas S, Laufman L, Hutchins L, Dickler M, et al. Multicenter phase II study of oral bexarotene for patients with metastatic breast cancer. J Clin Oncol 2003;21:999–1006.
32. Waters AM, Stewart JE, Atigadda VR, Mroczek-Musulman E, Muccio DD, Grubbs CJ, et al. Preclinical evaluation of a novel RXR agonist for the treatment of neuroblastoma. Mol Cancer Ther 2015;14:1559–69.
33. Waters AM, Stewart JE, Atigadda VR, Mroczek-Musulman E, Muccio DD, Grubbs CJ, et al. Preclinical evaluation of UAB30 in pediatric renal and hepatic malignancies. Mol Cancer Ther 2016;15:911–21.
34. Chou CF, Hsieh YH, Grubbs CJ, Atigadda VR, Mobley JA, Dummer R, et al. The retinoid X receptor agonist, 9-cis UAB30, inhibits cutaneous T-cell lymphoma proliferation through the SKP2-p27kip1 axis. J Dermatol Sci 2018;90:343–56.
35. Vuligonda V, Thacher SM, Chandraratna RA. Enantioselective syntheses of potent retinoid X receptor ligands: differential biological activities of individual antipodes. J Med Chem 2001;44:2298–303.
36. Kabbinavar FF, Zomorodian N, Rettig M, Khan F, Greenwald DR, Davidson SJ, et al. An open-label phase II clinical trial of the RXR agonist IRX4204 in taxane-resistant, castration-resistant metastatic prostate cancer (CRPC). J Clin Oncol 32:4s, 2014 (suppl; abstr 169).
37. Balasubramanian S, Chandraratna RAS, Eckert RL. Suppression of human pancreatic cancer cell proliferation by AGN194204, an RXR-selective retinoid. Carcinogenesis 2004;25:1377–85.
38. Lewis MT, Porter WW. Methods in mammary gland biology and breast cancer research: an update. J Mammary Gland Biol Neoplasia 2009;14:365.
39. Chou T, Martin N. CompuSyn for drug combinations: PC software and user's guide: a computer program for quantitation of synergism and antagonism in drug combinations, and the determination of IC_{50} and ED50 and LD50 values. Paramus, NJ: ComboSyn Inc; 2005.
40. Zheng S, Wang W, Aldahdooh J, Malyutina A, Shadbahr T, Tanoli Z, et al. SynergyFinder plus: toward better interpretation and annotation of drug combination screening datasets. Genomics Proteomics Bioinformatics 2022; 20:587–96.
41. Xu X, Wagner KU, Larson D, Weaver Z, Li C, Ried T, et al. Conditional mutation of Brca1 in mammary epithelial cells results in blunted ductal morphogenesis and tumour formation. Nat Genet 1999;22:37–43.
42. Li YX, Shen Q, Kim HT, Bissonnette RP, Lamph WW, Yan BF, et al. The rexinoid bexarotene represses cyclin D1 transcription by inducing the DEC2 transcriptional repressor. Breast Cancer Res Treat 2011;128:667–77.
43. Monaco ME. Fatty acid metabolism in breast cancer subtypes. Oncotarget 2017; 8:29487–500.
44. Kumar-Sinha C, Ignatoski KW, Lippman ME, Ethier SP, Chinnaiyan AM. Transcriptome analysis of HER2 reveals a molecular connection to fatty acid synthesis. Cancer Res 2003;63:132–9.
45. Menendez JA, Vellon L, Mehmi I, Oza BP, Ropero S, Colomer R, et al. Inhibition of fatty acid synthase (FAS) suppresses HER2/neu (erbB-2) oncogene overexpression in cancer cells. Proc Natl Acad Sci U S A 2004;101:10715–20.
46. Uray IP, Rodenberg JM, Bissonnette RP, Brown PH, Mancini MA. Cancer-preventive rexinoid modulates neutral lipid contents of mammary epithelial cells through a peroxisome proliferator-activated receptor gamma-dependent mechanism. Mol Pharmacol 2012;81:228–38.
47. Kamei Y, Miura S, Suganami T, Akaike F, Kanai S, Sugita S, et al. Regulation of SREBP1c gene expression in skeletal muscle: role of retinoid X receptor/liver X receptor and forkhead-O1 transcription factor. Endocrinology 2008;149: 2293–305.
48. Leal AS, Moerland JA, Zhang D, Carapellucci S, Lockwood B, Krieger-Burke T, et al. The RXR agonist MSU42011 is effective for the treatment of preclinical HER2+ breast cancer and kras-driven lung cancer. Cancers 2021;13:5004.
49. Reich LA, Moerland JA, Leal AS, Zhang D, Carapellucci S, Lockwood B, et al. The rexinoid V-125 reduces tumor growth in preclinical models of breast and lung cancer. Sci Rep 2022;12:293.
50. Feng WW, Wilkins O, Bang S, Ung M, Li J, An J, et al. CD36-mediated metabolic rewiring of breast cancer cells promotes resistance to HER2-targeted therapies. Cell Rep 2019;29:3405–20.
51. Vazquez-Martin A, Colomer R, Brunet J, Lupu R, Menendez JA. Overexpression of fatty acid synthase gene activates HER1/HER2 tyrosine kinase receptors in human breast epithelial cells. Cell Prolif 2008;41:59–85.
52. Piccinin E, Cariello M, Moschetta A. Lipid metabolism in colon cancer: role of liver X receptor (LXR) and Stearoyl-CoA desaturase 1 (SCD1). Mol Aspects Med 2021;78:100933.
53. Wang B, Tontonoz P. Liver X receptors in lipid signalling and membrane homeostasis. Nat Rev Endocrinol 2018;14:452–63.
54. Varga T, Czimmerer Z, Nagy L. PPARs are a unique set of fatty acid regulated transcription factors controlling both lipid metabolism and inflammation. Biochim Biophys Acta 2011;1812:1007–22.
55. Munir MT, Ponce C, Santos JM, Sufian HB, Al-Harrasi A, Gollahon LS, et al. VD (3) and LXR agonist (T0901317) combination demonstrated greater potency in inhibiting cholesterol accumulation and inducing apoptosis via ABCA1-CHOP-BCL-2 cascade in MCF-7 breast cancer cells. Mol Biol Rep 2020;47:7771–82.
56. Jiao XX, Lin SY, Lian SX, Qiu YR, Li ZH, Chen ZH, et al. The inhibition of the breast cancer by PPARgamma agonist pioglitazone through JAK2/STAT3 pathway. Neoplasma 2020;67:834–42.
57. Yao PL, Morales JL, Zhu B, Kang BH, Gonzalez FJ, Peters JM. Activation of peroxisome proliferator-activated receptor-beta/delta (PPAR-beta/delta) inhibits human breast cancer cell line tumorigenicity. Mol Cancer Ther 2014;13: 1008–17.
58. Flor AC, Wolfgeher D, Wu D, Kron SJ. A signature of enhanced lipid metabolism, lipid peroxidation and aldehyde stress in therapy-induced senescence. Cell Death Discov 2017;3:17075.
59. Shimizu R, Kanno K, Sugiyama A, Ohata H, Araki A, Kishikawa N, et al. Cholangiocyte senescence caused by lysophosphatidylcholine as a potential implication in carcinogenesis. J Hepatobiliary Pancreat Sci 2015;22:675–82.
60. Wang E. Senescent human fibroblasts resist programmed cell death, and failure to suppress bcl2 is involved. Cancer Res 1995;55:2284–92.

61. McDermott MSJ, Conlon N, Browne BC, Szabo A, Synnott NC, O'Brien NA, et al. HER2-targeted tyrosine kinase inhibitors cause therapy-induced-senescence in breast cancer cells. Cancers 2019;11:197.
62. Duro-Sanchez S, Nadal-Serrano M, Lalinde-Gutierrez M, Arenas EJ, Bernado Morales C, Morancho B, et al. Therapy-induced senescence enhances the efficacy of HER2-targeted antibody-drug conjugates in breast cancer. Cancer Res 2022; 82:4670–9.
63. Leal AS, Zydeck K, Carapellucci S, Reich LA, Zhang D, Moerland JA, et al. Retinoid X receptor agonist LG100268 modulates the immune microenvironment in preclinical breast cancer models. NPJ Breast Cancer 2019;5:39.
64. Bhargava P, Rathnasamy N, Shenoy R, Gulia S, Bajpai J, Ghosh J, et al. Clinical profile and outcome of patients with human epidermal growth factor receptor 2-positive breast cancer with brain metastases: real-world experience. JCO Glob Oncol 2022;8:e2200126.
65. Wang S, Wen P, Wood S. Effect of LXR/RXR agonism on brain and CSF Abeta40 levels in rats. F1000Res 2016;5:138.
66. Brown P, Arun B, Miller A, Isaacs C, Gutierrez C, Huang J, et al. Abstract CN04-04: Phase II trial of bexarotene in women at high risk of breast cancer: comparison of protein and RNA biomarkers. Cancer Prev Res 2008;1: CN04-04.